35th Annual International Conference of the IEEE EMBS
Osaka, Japan, 3 - 7 July, 2013

Blind Source Separation of Neural Activities from Magnetoencephalogram in Periodical Median Nerve Stimuli

Kuinharu Kishida

Abstract— **Neural activities of cortices in periodical median nerve stimuli are studied from magnetoencephalogram. The fractional type of the decorrelation method is used for the blind source separation with temporal structure. The blind source separation method is proposed for selecting neural activities related to somatosensory stimulus from magnetoencephalogram by comparing cross-correlation functions between components of blind source separation.**

I. INTRODUCTION

Somatosensory activities are known as the primary somatosensory cortex in the contralateral hemisphere (cSI), bilateral secondary somatosensory cortices (SIIs) and posterior parietal cortices in somatosensory stimuli with interstimulus intervals (ISIs) of more than one second [1], and the somatosensory activity is mainly observed at cSI in more than 3 Hz periodic median nerve stimulus [1], [2]. The effect of ISI upon brain information processing is important.

In the paper [3], responses of evoked magnetic fields were studied for 5Hz periodical median nerve stimuli. In 5Hz periodical median nerve stimulus, there are line peaks at 5Hz and its higher harmonic frequencies in the power spectral density (PSD) of the somatosensory evoked field (SEF). This suggests that averaged waveforms are deterministic. Statistical properties of SEF were summarized in [3] as SEF includes the deterministic part of concatenate averaged waveforms and the random part of fluctuations around them. Since lots of brain activities are included in magnetoencephalogram (MEG) data, neural activities are studied for the 2Hz periodical median nerve stimuli in the present paper.

The fractional type of the decorrelation method has been used for the blind source separation with temporal structure. When one forces the blind source separation (BSS) method to analyze MEG data, there are usually two serious consequences: 1) The signal from a single brain source may be divided into multiple BSS components. 2) One BSS component may contain signals from multiple brain sources. The blind source separation method will be examined for selecting neural activities related to somatosensory stimulus from magnetoencephalogram by comparing cross-correlation functions between components of blind source separation. Hence, neural activities of cortices in periodical median nerve stimuli can be studied from magnetoencephalogram.

* This research was supported by Grant-in-Aid for Scientific Research (No.22500254) of Japan society for the Promotion of Science.

Department of Department of Electrical, Electronic and Computer Engineering, Faculty of Engineering, Gifu University, Yanagido, Gifu, 501-1193 Japan kishida at gifu-u.ac.jp

II. ICA AND MEG

The decorrelation method [4], [5], [6] is one of independent component analyses (ICAs) and should be determined from simultaneous diagonalization of correlation matrices at all time delays. Let us assume that independent sources $\mathbf{s}(n)$ at time n are weakly stationary and observation $\mathbf{x}(n)$ with zero mean values is given by a mixing matrix A:

$$\mathbf{x}(n) = A\mathbf{s}(n), \tag{1}$$

where correlation matrix is written as

$$E\{\mathbf{x}(n)\mathbf{x}(n+m)^T\} = AE\{\mathbf{s}(n)\mathbf{s}(n+m)^T\}A^T = A\begin{pmatrix} C_{11}(m) & 0 & \dots & 0 \\ 0 & C_{22}(m) & \dots & 0 \\ \vdots & & \ddots & \vdots \\ 0 & \dots & 0 & C_{qq}(m) \end{pmatrix} A^T.$$

This procedure is theoretically attempted to remove the off-diagonal elements of correlation matrices at all time lags. Here the cross-correlation functions between ICA components are defined by

$$C_{ij}(m) := E\{s_i(n)s_j(m+n)\} = \frac{1}{N}\sum_{n=0}^{N-1} s_i(n)s_j(m+n). \tag{2}$$

The diagonal process can be approximately done in numerical calculations [7].

After minimization of a cost function by taking suitable repetition of Givens rotations of Jacobi algorithm correlation matrices of MEG in 2Hz median nerve stimuli can be written as

$$\mathbf{x}(n) = A^s\mathbf{s}_s(n) + A^e\mathbf{s}_e(n) + A^a\mathbf{s}_a(n), \tag{3}$$

where the subscripts s, e and a mean spontaneous magnetic fields, evoked magnetic fields and artifact noises respectively, if they are independent mutually. The ICA property has been used for artifact reduction in MEG data [5].

III. BSS AND MEG

The temporal decorrelation method has an open problem in choice of the time lags [5], [8], [9], [10]. The independent nature of the decorrelation method does not hold at particular time delays (see Section IV). Hence, the decorrelation method can be used for ICA or for BSS according to the choice of the time lags in numerical calculations. Since the performance of the decorrelation method is strongly dependent on the choice of time lag, then we will use the decorrelation method for BSS rather than for ICA to study intracerebral communications in the MEG analysis hereafter.

Since PSD of MEG with 1250Hz sampling frequency has a line spectrum of 2Hz and its higher harmonic modes in 2Hz periodical median nerve stimuli (see Fig. 1), improvements with the fractional type time lag τ_m defined by

$$\tau_m = \left(\frac{1250}{2}\right)/m = \frac{625}{m}, \quad m = 1, 2, \ldots, k, \qquad (4)$$

could be made by the decorrelation method [3], [10], [11]. Hence, we can determine a mixing matrix $A_{(k)}$ by the blind source separation with the T/k type (fractional) time lag of Eq. (4):

$$\mathbf{x}(n) = A_{(k)}\mathbf{s}^{(k)}(n). \qquad (5)$$

Eq. (5) was called the Tk type of BSS [11].

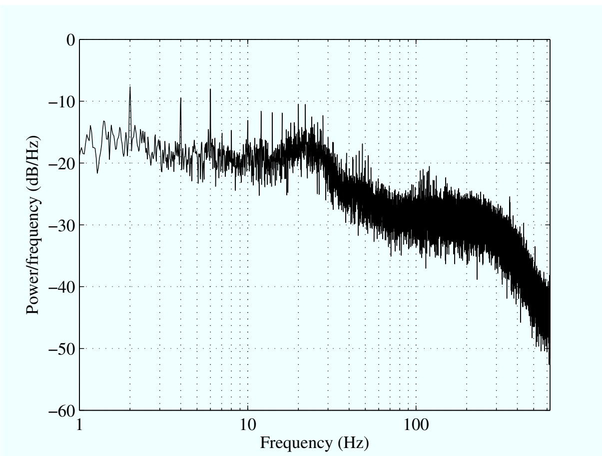

Fig. 1. PSD of the 22rd BSS component of Eq. (13).

The main processing in the decorrelation method is to remove the off-diagonal elements of the correlation matrices at fractional type time lag τ_m,

$$R_{zz}(\tau_m) = \frac{1}{N}\sum_{n=0}^{N-1} \boldsymbol{z}(n)\boldsymbol{z}(n+\tau_m)^T \quad m = 1, \ldots, k, \quad (6)$$

where the superscript T denotes the transposition of matrix and $\boldsymbol{z}(n)$ with zero mean is orthonormalized as $\sqrt{V^{-1}}\mathbf{x}(n)$. Here V is the covariance matrix given by $E\{\mathbf{x}(n)\mathbf{x}(n)^T\}$. In the T/k type of BSS, the sum of absolute squared off-diagonal elements of normalized correlation matrices is minimized at times corresponding to 2Hz and its higher harmonic frequencies, though the absolute sum of off-diagonal elements is minimized in ICA. The Jacobi-like algorithm has been used to approximately solve the simultaneous diagonalization problem on k normalized correlation matrices [7]. This process is to determine a square matrix U in the problem of minimization of the cost function J,

$$J(U) = \sum_{m=1}^{k}\sum_{i\neq j} |(UR_{zz}(\tau_m)U^T)_{ij}|^2, \qquad (7)$$

where $(UR_{zz}(\tau_m)U^T)_{ij}$ denotes the ij-element of matrix $UR_{zz}(\tau_m)U^T$. Finally, we have $A_{(k)}^{-1} := U\sqrt{V^{-1}}$. In the correlation matrices of Eq. (6), the stationarity is assumed in the decorrelation method. For achieving the stationarity, it should be noted that time series data were set to be zero mean in the interval between stimuli.

In the T/k type of BSS we must determine the k value. Firstly, an initial value of k may be determined from the number of peaks in PSD (see Fig. 1). Next, let us set k by half of the initial value and/or the double of it, and select the better value among three possible k-values in which clearer dipole patterns are found by examination of topographic field maps. If the choice is not enough, try setting of another k-value again. In this way we have selected a suitable k value $k = 30$ for 2Hz median nerve stimuli.

IV. Band Diagonalization and T/K Type of BSS

Van Kampen [12] developed the method of system size expansion using the scaling relation in order to understand the asymptotic nature of a macroscopic system far from equilibrium. In a normal case, macroscopic variables are divided into the most probable path and its fluctuation part:

$$\mathbf{x}(t) = \mathbf{u}(t) + \frac{1}{\sqrt{\Omega}}\mathbf{v}(t), \qquad (8)$$

where Ω is the system size. $\mathbf{u}(t)$ is described by a deterministic time-evolution equation and $\mathbf{v}(t)$ are macroscopic fluctuations. Fluctuations satisfy a linear Fokker-Planck equation in the normal scaling case [12], [13], [14], [15], which can be transformed into an equivalent linear Langevin equation:

$$\frac{d}{dt}\mathbf{v}(t) = \mathsf{L}\mathbf{v}(t) + \mathbf{r}(t), \qquad (9)$$

where $\mathbf{r}(t)$ are random forces and L is a constant matrix. Neural activities generated by group of neurons can be observed by superconducting quantum interference devices (SQUIDs). This means observed magnetic fields are macroscopic variables. Taking advantage of the macroscopic nature of asymptotic property, we can use this nature of the normal case from the viewpoint of statistical physics. In the measurement process, observation is given by $\mathbf{y}(t) = H\mathbf{v}(t)$. Here H is a constant matrix. It is expected in the normal case that fluctuations around the most probable path have the same temporal structure from Eq. (8). Since there are line spectrums in 2Hz periodical median nerve stimuli (see Fig. 1), fluctuations also have the same temporal structure relevant to line spectrums in the normal case.

In the discrete time representation Eq. (9) with the observation can be expressed theoretically [16] and numerically [17] in the Markov representation [18], [19]:

$$\begin{aligned} \mathbf{w}(n|n) &= \Phi\mathbf{w}(n-1|n-1) + K\gamma(n) \\ \mathbf{y}(n) &= H\mathbf{w}(n|n), \end{aligned}$$

where Φ and K are constant matrices and $\gamma(n)$ is the innovation, $\gamma(n) := \mathbf{y}(n) - \mathbf{y}(n|n-1)$. The Markov representation is transformed into

$$G_p(z^{-1})^{-1}\mathbf{y}(n) = \gamma(n), \qquad (10)$$

where $G_p(z^{-1}) := H(I - \Phi z^{-1})^{-1}K$ and z^{-1} is the backward time shift operator in the discrete time representation.

Hence, fluctuations in the normal case can be identified with the linear stochastic model Eq. (10).

Let somatosensory induced fields be reconstructed from suitable T/k BSS components in 2Hz periodical median nerve stimuli, and let us identify them by a linear stochastic model with the transfer function matrix, $G_p(z^{-1})$, which has poles corresponding to peaks at 2Hz and its higher harmonic modes. Let $\det G_p(z^{-1}) := \frac{n(z^{-1})}{d(z^{-1})}$, then roots of $d(z^{-1}) = 0$ have the poles which generate line spectrums as in Fig. 1. From Eq. (10) the numerator of $\det G_p(z^{-1})^{-1}$ becomes a small value at times corresponding to 2Hz and its higher harmonic modes. This statement will be used in evaluation of Eq.(12).

In the T/k type of BSS, correlation matrices of MEG in 2Hz median nerve stimuli can be written by removing the off-diagonal elements of correlation matrices as

$$\begin{aligned} &(A_{(k)})^{-1} E\{\mathbf{x}(n)\mathbf{x}(n+\tau_m)^T\}(A_{(k)})^{-T} \\ &= E\{\mathbf{s}^{(k)}(n)\mathbf{s}^{(k)}(n+\tau_m)^T\} \\ &= P_{(k)} \begin{pmatrix} C_l^{(k)}(\tau_m) & 0 \\ 0 & C_d^{(k)}(\tau_m) \end{pmatrix} P_{(k)}^T, \end{aligned} \tag{11}$$

where $P_{(k)}$ is a permutation matrix, $C_l^{(k)}(\tau_m) := E\{\mathbf{s}_l^{(k)}(n)\mathbf{s}_l^{(k)}(n+\tau_m)^T\}$ and $C_d^{(k)}(\tau_m) := E\{\mathbf{s}_d^{(k)}(n)\mathbf{s}_d^{(k)}(n+\tau_m)^T\}$. Here the subscripts l and d mean phenomena by linear equations and by nonlinear equations: $\mathbf{x}(n) = A^l\mathbf{s}_l(n) + A^d\mathbf{s}_d(n)$. When L is the lead field from the current dipoles $\mathbf{Q}(n)$, we have $\mathbf{x}^{(k)}(n) := L\mathbf{Q}(n)$, and have

$$L\mathbf{Q}(n) = A_{(k)}^l \delta\mathbf{s}_l^{(k)}(n),$$

at intermediate stage in iteration of Givens rotations of the Jacobi-like algorithm. By comparison of Eq. (10) with

$$(A_{(k)}^l)^{-1} L\mathbf{Q}(n) = \delta\mathbf{s}_l^{(k)}(n), \tag{12}$$

we find correspondences between $(A_{(k)}^l)^{-1}L$ and $G_p(z^{-1})^{-1}$, if $\mathbf{Q}(n)$ and $\delta\mathbf{s}_l^{(k)}(n)$ correspond to $\mathbf{y}(n)$ and $\gamma(n)$. The numerator of $\det G_p(z^{-1})^{-1}$ becomes a small value at the time delays of the T/k type of BSS, and then the decorrelation method happens to lose efficiency in numerical calculations of simultaneous diagonalization, and makes band structure of correlation function matrices of BSS components. This will be shown in an example of Section V.

V. MEG Analysis

For a subject the median nerve was stimulated electrically with a constant voltage, square-wave pulse of 0.2 ms duration delivered at right wrist. Stimulus frequency was periodical 2Hz ($T = 500$ms) and stimulus intensity was adjusted to the lowest level that would produce a twitch of the thumb. MEG data were recorded by a 64-channel whole-head MEG system (NeuroSQUID Model 100; CTF Systems Inc.). SQUID was the axial gradiometer type. MEG data were digitized with 1250Hz sampling frequency ($f_s = 1250$) and filtered by a 300Hz low pass filter. MEG data ($N = 218750$) during 250sec were recorded. MEG data were recorded at Osaka University from the subject. Informed consent was obtained from the subject prior to participation in the experiment. The experimental procedures were in accordance with the Declaration of Helsinki. This study was also approved by the Medical Review Board of Gifu University.

In the MEG analysis it is important to have stationary MEG data from observed MEG data by using a pre-signal processing. Let the number of sampled data between periodical median nerve stimuli, L, and $M := N/L = 350$ was a repetition number of 2Hz periodical median nerve stimuli. The inter-stimulus interval (ISI) was 500ms, and $L = 625$, since the sampling time Δt was 0.8ms. For pre-signal processing of MEG data, the mean value in each interval (500ms) was set to zero instead of high pass filter. Let $\mathbf{x}(n), n = 1, \ldots, N$ be sampled MEG data of 64 SQUIDs ($q = 64$), i.e., $\mathbf{x} \in \mathbf{R}^{q \times N}$. By using the T/k type of BSS with $k = 30$ we have

$$\mathbf{x}(n) = A_{(30)}\mathbf{s}^{(30)}(n). \tag{13}$$

$\mathbf{s}_4^{(30)}(n)$ and $\mathbf{s}_{22}^{(30)}(n)$ are BSS components of cSI because of their position of dipole pattern on the topographic map.

Cross-correlation functions, $C_{22,i}(n)$ between $\mathbf{s}_{22}^{(30)}(n)$ and the other BSS component, $\mathbf{s}_i^{(30)}(n)$ are examined and shown in Fig. 2. Since cSI is expressed by two BSS components, there are correlations between them, and $C_{22,4}(n)$ is described by the bold solid line in Fig. 2. The 26th BSS component $\mathbf{s}_{26}^{(30)}(n)$ is α wave component due to 10 Hz peak structure of PSD, and $C_{22,26}(n)$ is shown by the bold broken line. The bold dotted line is for $C_{22,51}(n)$ and the bold chain line is also for $C_{22,59}(n)$, though they are unknown components with 2 or 4Hz peak structure of PSD.

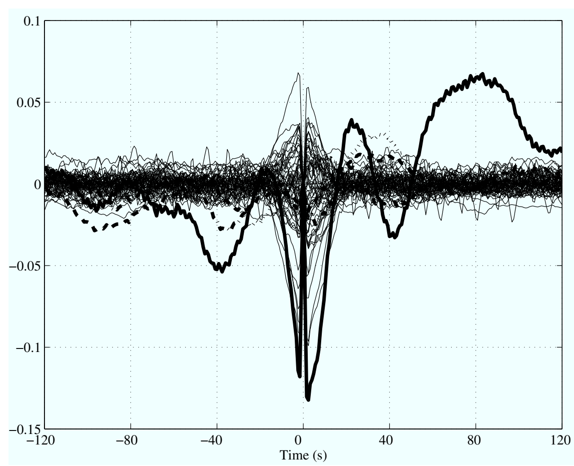

Fig. 2. Cross-correlation functions between the 22rd BSS component and the other BSS components.

Erasing $C_{22,4}(n)$, $C_{22,26}(n)$, $C_{22,51}(n)$ and $C_{22,59}(n)$ in Fig. 2 we can find remaining correlation functions in Fig. 3. In fig. 3 the 17th and 19th BSS components are eye movements or blinks because of their position of dipole pattern on the topographic map and their enhancement in the lower frequency region of PSD. $C_{22,17}(n)$ and $C_{22,19}(n)$

are shown by two bold solid lines. The bold broken lines of the 20th and 35th BSS components are also related to SIIs because of their position of dipole pattern on the topographic map. Two bold chain lines of the 24th and 30th BSS components are electrical power noises due to their time structure.

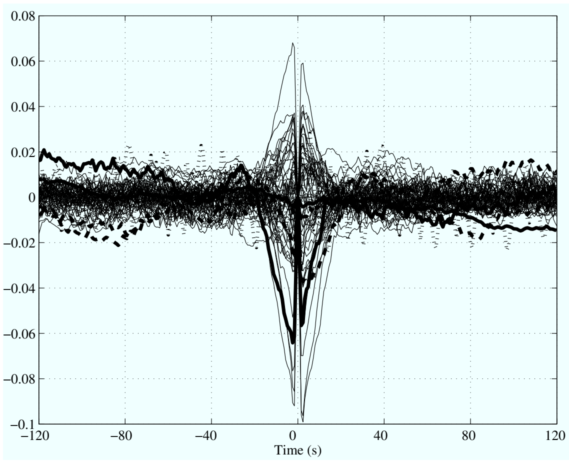

Fig. 3. Cross-correlation functions between the 22nd BSS component and the other BSS components with the exception of the 4th, 26th, 51st and 59th BSS components.

Erasing $C_{22,17}(n)$, $C_{22,19}(n)$, $C_{22,20}(n)$, $C_{22,24}(n)$, $C_{22,30}(n)$ and $C_{22,35}(n)$ in Fig. 3 we obtain still remaining correlation functions in Fig. 4. In Fig. 4 the bold solid line

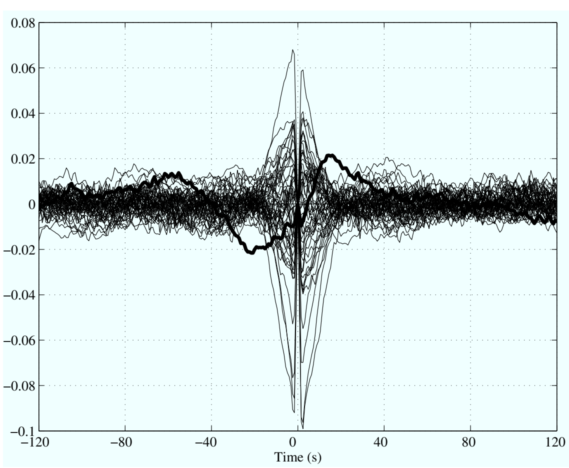

Fig. 4. Cross-correlation functions between the 22nd BSS component and the other BSS components with the exception of the 4th, 17th, 19th, 20th, 24th, 26th, 30th, 35th, 51st and 59thBSS components.

for $C_{22,3}(n)$ of the 3rd BSS component which is an unknown component with 4Hz peak structure of PSD.

When we eliminate $C_{22,3}(n)$ in Fig. 4, there remain small correlations among BSS components near the time origin, even if there is no small correlations among BSS components at certain times apart from the time origin. Therefore, correlation matrices of the fractional BSS components have band diagonal structure but not single diagonal.

VI. CONCLUSIONS

Neural activities of cortices in periodical median nerve stimuli were studied from magnetoencephalogram. The fractional type of the decorrelation method was used for the blind source separation with temporal structure. The blind source separation method was examined for selecting neural activities related to somatosensory stimulus from magnetoencephalogram by comparing cross-correlation functions between components of blind source separation. The blind source separation of neural activities from MEG data is useful to study intracerebral communications [11].

REFERENCES

[1] H. Wikström, J. Huttunen, A. Korvenoja, J. Virtanen, O. Salonen, H. Aronen, and R. J. Ilmonniemi, Effects of interstimulus interval on somatosensory evoked magnetic fields (SEFs): a hypothesis concerning SEF generation at the primary sensorimotor cortex, Electroencephalogr. Clin. Neurophysiol., vol. 100, pp. 479-487, 1996.

[2] Y. Hamada, S. Otsuka, T. Okamoto, and R. Suzuki, The profile of the recovery cycle in human primary and secondary somatosensory cortex: a magnetoencephalography study, Clin. Neurophysiol., vol. 113, pp. 1787-1793, 2002.

[3] K. Kishida, Evoked magnetic fields of magnetoencephalogrphy and their statistical property, Phys. Rev. E, vol. 79, pp. 011922 2009.

[4] L. Molgedey and H. G. Schuster, Separation of a mixture of independent signals using time delayed correlations, Phys. Rev. Lett., vol. 72, pp. 3634-3637, 1984.

[5] A. Ziehe, K. R. Müller, G. Nolte, B. M. Mackert, and G. Curio, Artifact reduction in magnetoneurography based on time-delayed second-order correlations, IEEE Trans. Biomed. Eng., vol. 47, pp. 75-87, 2000.

[6] N. Murata, S. Ikeda, and A. Ziehe, An approach to blind source separation based on temporal structure of speech signals, Neurocomputing, vol. 41, pp. 1-24, 2001.

[7] J. F. Cardoso and A. Souloumiac, Jacobi angles for simultaneous diagonalization, SIAM J. Mat. Anal. Aplpl., vol. 17, pp. 161-163, 1996.

[8] A. C. Tang, M. T. Sutherland, and C. J. McKinney, Validation of SOBI components from high-density EEG, NeuroImage, vol. 25, pp. 539-553, 2005.

[9] N. Hironaga, and A. A. Ioannides, Localization of individual area neuronal activity, NeuroImage, vol. 34, pp. 1519-1534,2007.

[10] K. Kishida, Classification of activities related to 5Hz periodical median nerve stimuli by using the temporal decorrelation method of BSS, in Biomagnetism: Interdisciplinary Research and Exploration, R. Kakigi, K Yokosawa and S. Kuriki Ed.: Hokkaido University Press, 2008, pp. 124-126.

[11] K. Kishida, Intracerebral communication studied by magnetoencephalography. in Advances in Brain Imaging, V. Chaudhary Ed.: InTech, ch. 10, 2012, (pp. 195-220). (ISBN: 978-953-307-955-4).

[12] N.G. Van Kampen, A power series expansion of the master equation, Can. J. Phys. Vol. 39, pp. 551-567, 1961.

[13] R. Kubo, K. Matsuo, and K. Kitahara, Fluctuations and relaxation of macrovariables, J. Stat. Phys., vol. 9, pp. 51-96, 1973.

[14] K. Tomita and Tomita, Irreversible circulation of fluctuation, Prog. Theor. Phys., vol. 51, pp. 1731-1749, 1974.

[15] K. Kishida, S. Kanemoto, and T. Sekiya, Reactor noise theory based on system size expansion, J. Nucl. Sci. Technol., vol. 13, pp. 19-29, 1976.

[16] K. Kishida, Physical Langevin model and the time-series model in system far from equilibrium, Phys. Rev. A, vol. 25, pp. 496-507, 1982.

[17] K. Kishida, Contraction of information in systems far from equilibrium, J. Math. Phys., vol. 32, pp. 92-98, 1991.

[18] H. Akaike, Stochastic theory of minimal realization, IEEE Trans. Automatic Control, vol. 19, pp. 667-674, 1974.

[19] K. Kishida, Contraction of information and its inverse problem in reactor system identification, in Advances in Nuclear Science and Technology, Vol. 23, J. Lewins and M. Becker Ed. New York: Plenum Press 1996, pp. 1-68.